2-16-2018

The oligomerization state of bacterial enzyme I (EI) determines EI's allosteric stimulation or competitive inhibition by α-ketoglutarate

Trang T. Nguyen
Iowa State University, trangnt@iastate.edu

Rodolfo Ghirlando
National Institutes of Health

Vincenzo Venditti
Iowa State University, venditti@iastate.edu

The oligomerization state of bacterial enzyme I (EI) determines EI's allosteric stimulation or competitive inhibition by α-ketoglutarate

Abstract

The bacterial phosphotransferase system (PTS) is a signal transduction pathway that couples phosphoryl transfer to active sugar transport across the cell membrane. The PTS is initiated by phosphorylation of enzyme I (EI) by phosphoenolpyruvate (PEP). The EI phosphorylation state determines the phosphorylation states of all other PTS components and is thought to play a central role in the regulation of several metabolic pathways and to control the biology of bacterial cells at multiple levels, for example, affecting virulence and biofilm formation. Given the pivotal role of EI in bacterial metabolism, an improved understanding of the mechanisms controlling its activity could inform future strategies for bioengineering and antimicrobial design. Here, we report an enzymatic assay, based on Selective Optimized Flip Angle Short Transient (SOFAST) NMR experiments, to investigate the effect of the small-molecule metabolite α-ketoglutarate (αKG) on the kinetics of the EI-catalyzed phosphoryl transfer reaction. We show that at experimental conditions favoring the monomeric form of EI, αKG promotes dimerization and acts as an allosteric stimulator of the enzyme. However, when the oligomerization state of EI is shifted toward the dimeric species, αKG functions as a competitive inhibitor of EI. We developed a kinetic model that fully accounted for the experimental data and indicated that bacterial cells might use the observed interplay between allosteric stimulation and competitive inhibition of EI by αKG to respond to physiological fluctuations in the intracellular environment. We expect that the mechanism for regulating EI activity revealed here is common to several other oligomeric enzymes.

Keywords

allosteric regulation, inhibition mechanism, protein assembly, nuclear magnetic resonance (NMR), signaling, enzyme stimulation, protein oligomerization, SOFAST-TROSY

Disciplines

Biochemistry | Molecular Biology | Organic Chemistry

Comments

This article is published as Nguyen, Trang T., Rodolfo Ghirlando, and Vincenzo Venditti. "The oligomerization state of bacterial enzyme I (EI) determines EI's allosteric stimulation or competitive inhibition by α-ketoglutarate." *Journal of Biological Chemistry* 293, no. 7 (2018): 2631. DOI: 10.1074/jbc.RA117.001466.

The oligomerization state of bacterial enzyme I (EI) determines EI's allosteric stimulation or competitive inhibition by α-ketoglutarate

Received for publication, December 13, 2017, and in revised form, January 4, 2018 Published, Papers in Press, January 9, 2018, DOI 10.1074/jbc.RA117.001466

Trang T. Nguyen[‡], **Rodolfo Ghirlando**[§], **and Vincenzo Venditti**[‡¶1]

From the [‡]*Department of Chemistry and the* [¶]*Roy J. Carver Department of Biochemistry, Biophysics and Molecular Biology, Iowa State University, Ames, Iowa 50011 and the* [§]*Laboratory of Molecular Biology, NIDDK, National Institutes of Health, Bethesda, Maryland 20892*

Edited by Wolfgang Peti

The bacterial phosphotransferase system (PTS) is a signal transduction pathway that couples phosphoryl transfer to active sugar transport across the cell membrane. The PTS is initiated by phosphorylation of enzyme I (EI) by phosphoenolpyruvate (PEP). The EI phosphorylation state determines the phosphorylation states of all other PTS components and is thought to play a central role in the regulation of several metabolic pathways and to control the biology of bacterial cells at multiple levels, for example, affecting virulence and biofilm formation. Given the pivotal role of EI in bacterial metabolism, an improved understanding of the mechanisms controlling its activity could inform future strategies for bioengineering and antimicrobial design. Here, we report an enzymatic assay, based on Selective Optimized Flip Angle Short Transient (SOFAST) NMR experiments, to investigate the effect of the small-molecule metabolite α-ketoglutarate (αKG) on the kinetics of the EI-catalyzed phosphoryl transfer reaction. We show that at experimental conditions favoring the monomeric form of EI, αKG promotes dimerization and acts as an allosteric stimulator of the enzyme. However, when the oligomerization state of EI is shifted toward the dimeric species, αKG functions as a competitive inhibitor of EI. We developed a kinetic model that fully accounted for the experimental data and indicated that bacterial cells might use the observed interplay between allosteric stimulation and competitive inhibition of EI by αKG to respond to physiological fluctuations in the intracellular environment. We expect that the mechanism for regulating EI activity revealed here is common to several other oligomeric enzymes.

Enzyme I (EI)[2] is the first protein of the bacterial phosphotransferase system (PTS), a signal transduction pathway that results in active sugar transport across the cell membrane (1–3). The PTS is initiated by phosphorylation of EI by the small molecule phosphoenolpyruvate (PEP). Phosphorylated EI transfers the phosphoryl group to the phosphocarrier protein HPr. Thereafter, the phosphoryl group is transferred to a sugar-specific enzyme II and finally to the incoming sugar (Fig. 1*a*). Recently, the small-molecule metabolite α-ketoglutarate (αKG) was shown to act as a competitive inhibitor of EI (inhibition constant, $K_I = \sim 2.2$ mM) (4, 5). The intracellular concentration of αKG varies considerably in response to a change in the availability of nitrogen source in the culturing medium (from 0.5 mM, in the presence of 10 mM NH_4Cl, to 10 mM, in the absence of nitrogen source) (4). Thus, inhibition of EI by αKG has been proposed as a biochemical mechanism that links the uptake of sugars to the availability of nitrogen source (4, 5). In addition to playing a primary role in coupling carbon and nitrogen metabolism in bacteria, the phosphorylation state of EI strictly controls the phosphorylation state of all other PTS components (6), which in turn regulates a large number of bacterial functions, including catabolic gene expression, virulence, biofilm formation, chemotaxis, potassium transport, and inducer exclusion, via phosphorylation-dependent protein-protein interactions (2). Therefore, EI is a central regulator of bacterial metabolism, and obtaining a comprehensive understanding of the mechanisms tuning its biological activity may suggest new strategies in bioengineering and antimicrobial design and might help elucidating the coupling between metabolic networks that controls the biology of all living cells.

EI is a multidomain protein comprising a N-terminal domain (EIN, residues 1–249) that contains the phosphorylation site (His^{189}) and the binding site for HPr and a C-terminal domain (EIC, residues 261–575) that is responsible for protein dimerization and contains the binding site for PEP and the competitive inhibitor αKG. The EIN and EIC domains are connected by a short helical linker (residues 250–260) (1, 7). EI undergoes a series of large-scale conformational rearrangements during its catalytic cycle (Fig. 1*b*), including: (i) a monomer–dimer transition (8), (ii) an expanded-to-compact conformational change within EIC (9), and (iii) an open-to-close transition describing a reorientation of EIN relative to EIC (10–12). PEP binding to EIC shifts the conformational equilibria toward the catalytically competent dimer/compact/close form and activates the enzyme for catalysis (Fig. 1*b*) (11). The mono-

This work was supported by funds from the Roy J. Carver Charitable Trust and Iowa State University (to V. V.) and by the Intramural Research Program of the NIDDK, National Institutes of Health (to R. G.). The authors declare that they have no conflicts of interest with the contents of this article. The content is solely the responsibility of the authors and does not necessarily represent the official views of the National Institutes of Health.

[1] To whom correspondence should be addressed: Dept. of Chemistry, Iowa State University, Ames, Iowa 50011. Tel.: 515-294-1044; Fax: 515-294-7550; E-mail: venditti@iastate.edu.

[2] The abbreviations used are: EI, enzyme I; αKG, α-ketoglutarate; PTS, phosphotransferase system; PEP, phosphoenolpyruvate; EIN, EI N-terminal domain; EIC, EI C-terminal domain; AUC, analytical ultracentrifugation; TROSY, transverse relaxation optimized spectroscopy; SOFAST, Selective Optimized Flip Angle Short Transient.

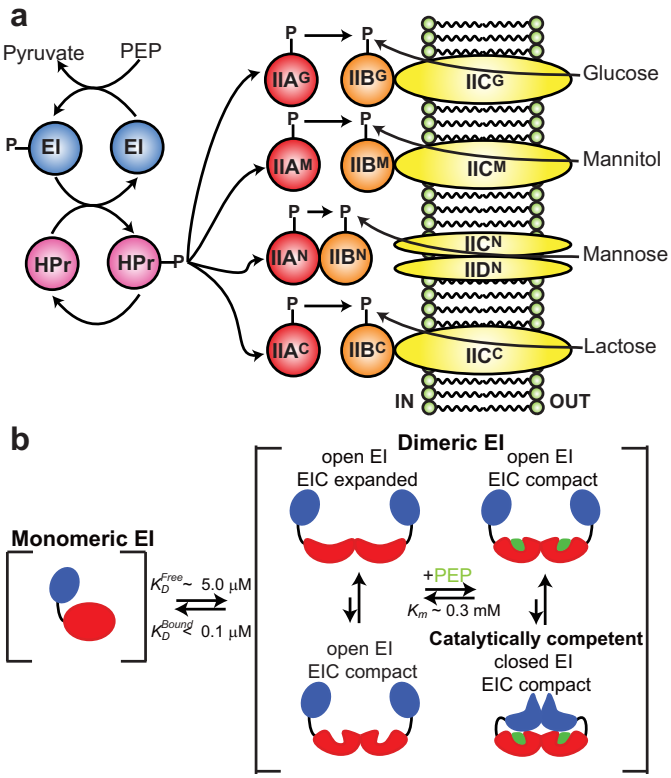

Figure 1. The bacterial PTS. *a*, diagram of the *E. coli* PTS. The first two steps are common to all branches of the pathway. Thereafter, the pathway splits into four sugar-specific classes: glucose, mannitol, mannose, and lactose/chitobiose. *Blue*, EI; *pink*, HPr; *red*, enzyme IIA; *orange*, enzyme IIB; *yellow*, enzyme IIC/enzyme IID. EIIC/EIID enzymes are shown in a lipid bilayer. The phosphorylated site is indicated by *P*. *b*, schematic summary of the conformational equilibria of EI during its catalytic cycle. The EIN domain is colored *blue*, the EIC domain is colored *red*, and PEP is colored *green*. Equilibrium constants reported in previous research articles (5, 8) are shown. K_D^{Free} and K_D^{Bound} are the equilibrium dissociation constants for dimerization in the absence and in the presence of saturating concentrations of Mg^{2+} and PEP, respectively.

mer–dimer equilibrium of EI has been often suggested as a major regulatory element for PTS because (i) only dimeric EI can be phosphorylated by PEP (13): (ii) the interaction of the enzyme with its physiological ligands Mg^{2+} and PEP (Michaelis constant, K_m, measured in the presence of 4 mM Mg^{2+} was ~300 μM) decreases the equilibrium dissociation constant for dimerization (K_D) by more than 10-fold (from ~5 to <0.1 μM) (5, 8); and (iii) the intracellular concentrations of EI and PEP were reported to vary substantially depending on the experimental conditions (from ~30 to ~300 μM for PEP and from ~1 to ~10 μM for EI) (14–16).

Here, we develop a flexible enzymatic assay to investigate the effect of perturbations of the monomer–dimer equilibrium of *Escherichia coli* EI on the activity of αKG against the enzyme. We show that at physiological concentrations of EI and PEP that promote dimerization of EI ([EI] > K_D, [PEP] > K_m), αKG acts as a competitive inhibitor of EI. In contrast, at physiological conditions favoring the monomeric form of the enzyme ([EI] < K_D, [PEP] < K_m), αKG allosterically stimulates EI autophosphorylation. To our knowledge, this is one of the few examples of a small molecule metabolite being reported to both inhibit and stimulate the activity of the same enzyme depending on the experimental conditions (the other known case is ATP that can be a substrate or an allosteric inhibitor of phosphofructokinase) (17). The fact that the intracellular concentrations of EI, PEP, and αKG are modulated by the composition of the culturing medium (4, 14–16) suggests that this interplay between allosteric stimulation and competitive inhibition of EI might be used by bacterial cells to regulate the phosphorylation state of PTS in response to a change in the extracellular environment.

Results

Effect of PEP and αKG on the monomer–dimer equilibrium of EI

The effect of the EI ligands, PEP and αKG, on the monomer–dimer equilibrium of the enzyme was investigated by analytical ultracentrifugation (AUC). The sedimentation velocity data indicate that the monomer–dimer equilibrium of EI is shifted toward the monomeric species at concentrations of the enzyme of <1 μM (Fig. 2*a*) and that addition of PEP or αKG results in a substantial stabilization of the dimeric state (Fig. 2, *b* and *c*). Our results are consistent with the more than 10-fold decrease in dimerization K_D reported previously for EI upon addition of PEP or αKG (5, 8).

Kinetics of the phosphoryl transfer reaction

The addition of 10 mM PEP to a NMR sample containing 1 mM ^{15}N-labeled *E. coli* HPr and ~0.05 μM *E. coli* EI (unlabeled) results in substantial chemical shift perturbations for the ^{1}H–^{15}N transverse relaxation optimized spectroscopy (TROSY) (18) peaks originating from HPr residues located in the vicinity of the phosphorylation site (His^{15}; Fig. 3, *a* and *c*). As previously noted, HPr does not interact directly with PEP, nor can it be phosphorylated in the absence of EI (19). Therefore, the observed spectral changes are attributed to HPr phosphorylation via EI. After 24 h of incubation at 37 °C, the HPr spectrum relaxes back to the unphosphorylated form (Fig. 3*a*), which is consistent with the low thermodynamic stability of phosphorylated histidine residues (20).

Here, we use ^{1}H-^{15}N SOFAST-TROSY spectra (21) to monitor the time evolution of the phosphoryl transfer reaction from PEP to HPr via EI. SOFAST NMR experiments are ideally suited for real-time investigations on reaction kinetics, because they allow acquisition of 2D NMR spectra within seconds (21). For this particular case, ~0.05 μM unlabeled EI and 1 mM ^{15}N-labeled HPr are mixed in 500 μl of reaction buffer (see "Experimental procedures") and incubated at 37 °C for 30 min in a conventional 5-mm NMR tube. Thereafter, the reaction is started by addition of the desired amount of PEP (note that the PEP stock solution is preincubated at 37 °C). The sample is mixed in the NMR tube and equilibrated at 37 °C for 1 min in the NMR magnet. The reaction is then monitored for 20 min by running a series of 2D ^{1}H-^{15}N SOFAST-TROSY spectra (1 min each). The phosphoryl transfer reaction is slow on the chemical-shift time scale, and distinct NMR peaks are observed for the phosphorylated and unphosphorylated species (Fig. 3*b*). To monitor the evolution of the phosphoryl transfer reaction, we have used the NMR peak intensities of residues Ala^{10}, Gly^{13}, and Gly^{54} because they are characterized by high signal-to-noise ratio and are well resolved throughout the experiment

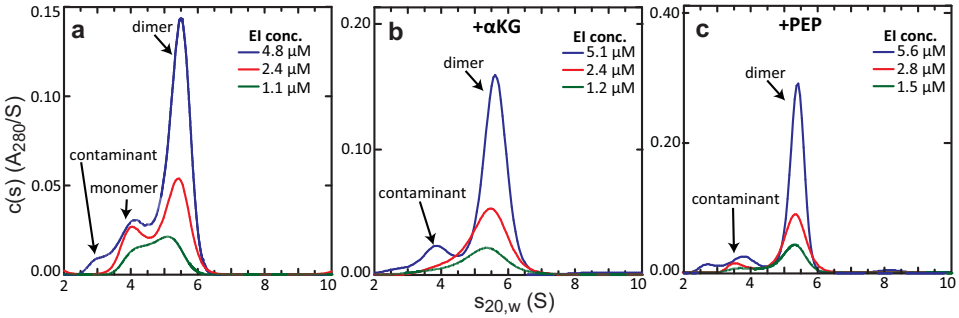

Figure 2. PEP and αKG shift the monomer–dimer equilibrium of EI. *c*(*s*) distributions for EI obtained at different loading concentrations (ranging from ~5 to ~1 μM) based on sedimentation velocity absorbance data collected at 50 kilo-revolutions per minute and 20.0 °C (see "Experimental procedures"). *a*, data acquired for the free EI revealed concentration-dependent *c*(*s*) absorbance profiles typical of a monomer–dimer equilibrium. *b* and *c*, in the presence of 20 mM αKG (*b*) and 20 mM PEP (*c*), the sedimentation experiments indicate that EI is dimeric within the tested concentration range. Peaks at $s_{20,w}$ <4 S that do not show concentration dependent *c*(*s*) absorbance profiles (*i.e.* they do not report on the monomer–dimer equilibrium) are attributed to small amounts of contaminants in the AUC sample.

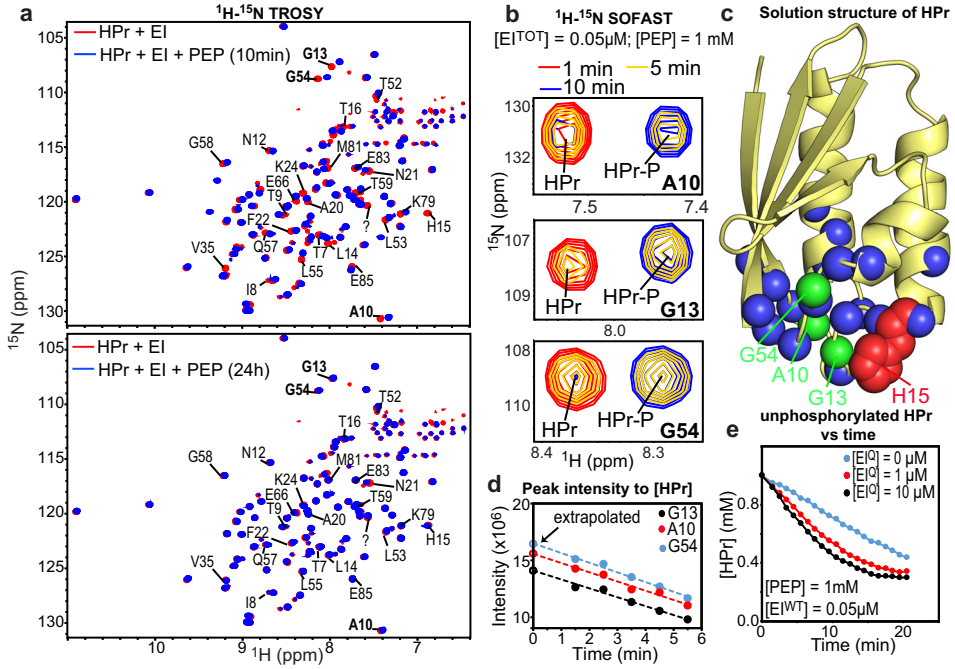

Figure 3. Activity assay for the phosphoryl transfer reaction. *a*, ^{1}H-^{15}N TROSY spectrum of ^{15}N-labeled HPr in the presence of 0.05 μM unlabeled EI in the absence (*red*) and in the presence (*blue*) of 10 mM PEP. Spectra in the presence of PEP were measured after incubation for 10 min (*upper panel*) or 24 h (*lower panel*) at 37 °C. Cross-peaks showing chemical shift perturbation upon addition of PEP are labeled. The *question mark* indicates a peak of unknown assignment. *b*, close-up views of a ^{1}H-^{15}N SOFAST-TROSY spectrum of 1 mM HPr in the presence of 0.05 μM EI and 1 mM PEP showing the cross-peaks for residues Ala^{10}, Gly^{13}, and Gly^{54} at three different time points during the activity assay: 1 min (*red*), 5 min (*yellow*), and 10 min (*blue*). For each residue, distinct peaks are observed for the unphosphorylated and phosphorylated HPr species (labeled HPr and HPr-P in the figure, respectively). *c*, 3D structure of HPr. Backbone amide groups experiencing chemical shift perturbation upon addition of PEP to a sample containing HPr and EI are shown as *spheres*. Amide groups for Ala^{10}, Gly^{13} and Gly^{54} are colored *green*. The phosphorylation site (His^{15}) is shown as *red spheres*. *d*, intensities of the ^{1}H-^{15}N SOFAST-TROSY cross-peaks of Ala^{10} (*red*), Gly^{13} (*black*) and Gly^{54} (*blue*) are plotted *versus* time. Intensities at time 0 were obtained by extrapolation. The displayed data were measured on a 1 mM sample of HPr containing 0.05 μM EI^{WT} and 1 mM PEP. The extrapolated intensities at time 0 (corresponding to 1 mM HPr) were used to calculate the time dependence of the unphosphorylated HPr concentration. *e*, the concentration of unphosphorylated HPr is plotted *versus* time. The displayed data were measured on a 1 mM sample of HPr containing 0.05 μM EI^{WT} and 1 mM PEP. Concentrations of EI^{Q} were 0 (*blue*), 1 (*red*), and 10 μM (*black*).

(Fig. 3*b*). Because the early time points are more important in determining the initial rate of the reaction, we limited our analysis to the disappearance of the unphosphorylated species, for which NMR peaks with high signal-to-noise ratios are obtained at the beginning of the phosphoryl transfer reaction (note the phosphorylated HPr peaks are not present at time zero; Fig. 3*b*). Signal intensities are plotted *versus* time, and the linear portion of the decay is fit to obtain the initial rate of change (Fig. 3*d*). To convert the reaction rate from change in signal intensity over time to change in concentration of unphosphorylated HPr over time, the NMR signal intensities at time zero for Ala^{10}, Gly^{13}, and Gly^{54} were obtained by extrapolation (Fig. 3*d*) and considered to correspond to the expected signal intensity for a 1 mM HPr sample. Unphosphorylated HPr concentration at any time point is reported as the average over the three analyzed peaks (Fig. 3*e*).

To evaluate the effect of an increased concentration of dimeric EI on the activity of the enzyme, enzyme kinetic data were collected at a fixed concentration of EI (~0.05 μM), PEP (1 mM), and HPr (1 mM), and with increasing concentration of the

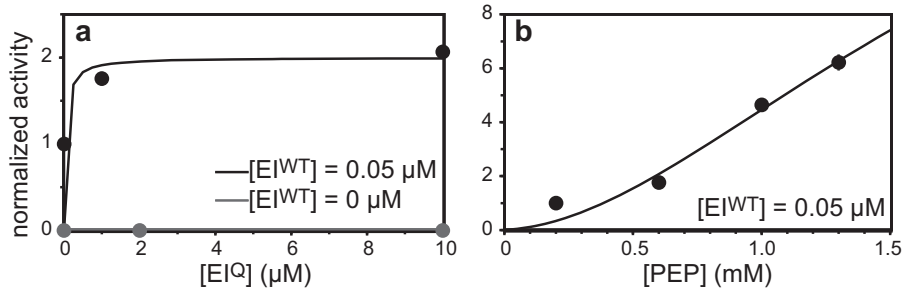

Figure 4. Dependence of the phosphoryl transfer reaction on the concentration of substrate and enzyme. *a*, the phosphoryl transfer activity of EI (measured in the presence of 1 mM PEP) is plotted *versus* the concentration of an inactive mutant of the enzyme (EI^Q) in the presence of 0 (*gray*) or 0.05 μM wildtype EI (EI^{WT}). The data were fit using the kinetic model summarized by Equations 1–12 ("Experimental procedures"). The results of the fits are shown as *solid lines*. *b*, the phosphoryl transfer activity of EI is plotted *versus* the concentration of PEP. The data were fit using the kinetic model summarized by Equations 13–20 ("Experimental procedures"). The results of the fits are shown as *solid lines*.

inactive EI mutant H189Q (EI^Q). His^{189} is located within the N-terminal domain of the enzyme and does not participate in the dimer interface or in PEP/αKG binding to EIC. Indeed, EI^Q has been recently reported to have the same equilibrium dissociation constant for dimerization and to form an identical EIC dimer as the wildtype EI (11, 22). Therefore, EI^Q cannot receive the phosphoryl group from PEP but can still interact with the wildtype protein (EI^{WT}) to form an active EI dimer. As expected, increasing the concentration of EI^Q from 0 to 10 μM doubles the HPr phosphorylation rate measured by our NMR assay (Fig. 4*a*). It is worth noticing that EI^Q is inactive in the absence of EI^{WT} (Fig. 4*a*). Therefore, the increased enzymatic activity observed by adding EI^Q to a sample with a low concentration of EI^{WT} (~0.05 μM) is due to an increased population of dimeric EI (which goes from 8% in the absence of EI^Q to 80% in the presence of 10 μM EI^Q) and not to the eventual presence of EI^{WT} contaminations in purified EI^Q. The dependence of the HPr phosphorylation rate on the total concentration of EI ($[EI^{TOT}] = [EI^{WT}] + [EI^Q]$) can be fit considering that (i) only dimeric EI can catalyze the phosphoryl transfer reaction (13), (ii) binding of PEP to both monomeric subunits results in stabilization of the EI dimer, and (iii) binding of PEP to one monomeric subunit affects the K_D for EI dimerization to a minor extent. To reduce the number of fitted parameters, we have assumed that the dimer K_D is not affected by binding of a single molecule of PEP to EI (see Equations 1–12 under "Experimental procedures"). The fit was performed in DynaFit 4.0 (23) by keeping K_m and K_D for the free enzyme ($K_{D,free}$) to their measured values (300 and 1 μM, respectively; note that the 5 μM value for $K_{D,free}$ reported in Fig. 1*b* was measured in the absence of Mg^{2+}) (5) and by optimizing the dissociation constant for the EI dimer saturated with PEP ($K_{D,bound}$) and the catalytic rate constant for phosphoryl transfer (k_{phosp}). The results of the fitting are shown in Fig. 4*a* and are consistent with the pronounced stabilization of the EI dimer induced by PEP binding observed by AUC experiments (fitted $K_{D,bound} < 10^{-7}$ M). A similar kinetic model (Equations 13–20 under "Experimental procedures") and the same equilibrium constants were used to fit the dependence of the rate of HPr phosphorylation on the concentration of PEP at a fixed concentration of enzyme (~0.05 μM; Fig. 4*b*). It is worth noticing that increasing the concentration of PEP beyond 1.3 mM makes the phosphoryl transfer reaction too fast to be monitored by our method at our experimental conditions (37 °C and ~0.05 μM enzyme). Therefore, k_{phosp} cannot be accurately determined by the available data. However, our fitted results ($k_{phosp} > 10{,}000\ s^{-1}$) are in good agreement with the fast conversion rates previously reported for the EI autophosphorylation reaction (24).

Effect of αKG on the activity of EI

The data reported in the previous sections indicate that dimerization stimulates the phosphoryl transfer activity of EI (Fig. 4*a*) and that increasing the concentration of αKG from 0 to 20 mM shifts the monomer–dimer equilibrium toward the enzymatically active EI dimer (Fig. 2). In this section, we evaluate the effect of αKG on the phosphoryl transfer activity of EI at experimental conditions that promote the monomeric or dimeric form of the enzyme.

At low concentration of enzyme ($<K_{D,free}$) and substrate ($<K_m$), we expect EI to exist predominantly as a monomer. In this case, the addition of small concentrations of αKG ($<K_I$) will act synergistically with PEP in saturating the binding sites on EI (Fig. 5*a*). The increased population of EI-ligand adducts will result in stabilization of the enzymatically active EI dimer and allosteric stimulation of the phosphoryl transfer reaction (Fig. 5*a*). In contrast, increasing the concentration of αKG to values larger than K_I will result in oversaturation of the binding sites on EI and consequential competitive inhibition of enzymatic activity (Fig. 5*a*). Indeed, enzyme kinetic data collected at ~0.05 μM EI, 200 μM PEP, and increasing concentrations of αKG (0–10 mM) show an initial stimulation of enzymatic activity followed by a decrease in the rate of phosphoryl transfer at high concentration of αKG (> 2 mM; Fig. 6*a*). At concentrations of EI > $K_{D,free}$ and/or concentrations of PEP > K_m, we expect EI to exists predominantly as a dimer, and αKG to act exclusively as an inhibitor of the enzyme (Fig. 5*b–d*). Experimental data collected at ~0.05 μM EI and 1000 μM PEP (Fig. 6*b*), at 10 μM EI and 200 μM PEP (Fig. 6*c*), and at 10 μM EI and 1000 μM PEP (Fig. 6*d*) confirm the expected behavior. Interestingly all kinetic data reported in Fig. 6 can be fit considering that (i) only dimeric EI can catalyze the phosphoryl transfer reaction (13), (ii) saturation of the EI dimer-binding sites with PEP and/or αKG (dissociation constants K_m and K_I, respectively) decreases the K_D for EI dimerization, and (iii) binding of PEP or αKG to one monomeric subunit affects the K_D for EI dimerization to a minor extent. As done in the previous section when

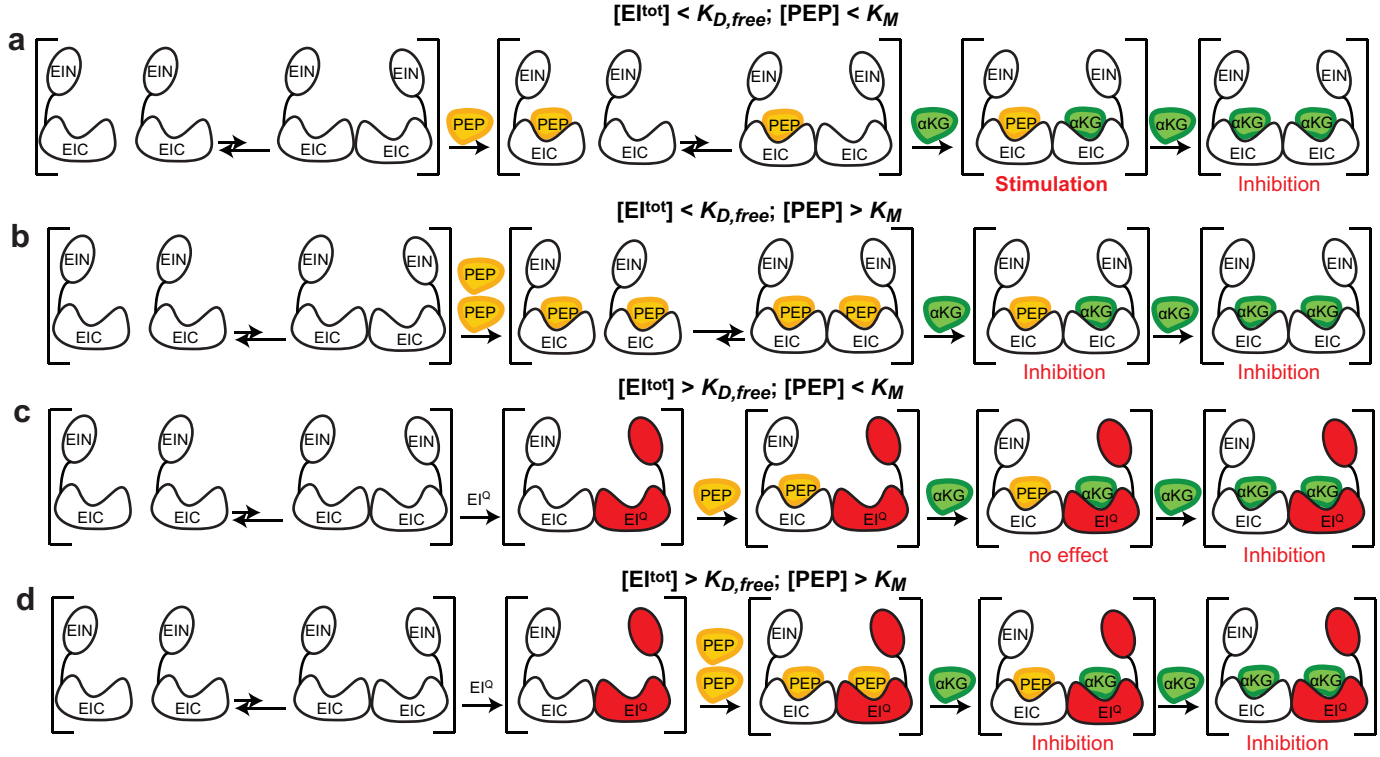

Figure 5. The monomer–dimer equilibrium of EI regulates the activity of αKG on the enzyme. *a*, at low concentration of enzyme ($< K_{D,free}$) and PEP ($< K_m$) addition of αKG stabilizes the catalytically active EI dimer and stimulates the activity of the enzyme. Increasing the concentration of αKG to values higher than K_I results in displacement of PEP from the active site and inhibition of EI. *b*, at a high concentration of PEP ($> K_m$), the addition of αKG does not affect the population of dimeric EI (which is already stabilized by PEP binding to both subunits) and results in inhibition of the enzyme. *c* and *d*, at an EI concentration larger than $K_{D,free}$, the monomer dimer equilibrium is already shifted toward the dimer form, and no stimulatory effect of αKG is detected at a low (*c*) or high (*d*) concentration of PEP. The total concentration of enzyme (EI^{TOT}) is the sum of the concentrations of the wildtype EI (EI^{WT}) and of an inactive EI mutant (EI^{Q}, see "Results"). PEP and αKG are colored *yellow* and *green*, respectively. EI^{WT} and EI^{Q} are colored *white* and *red*, respectively.

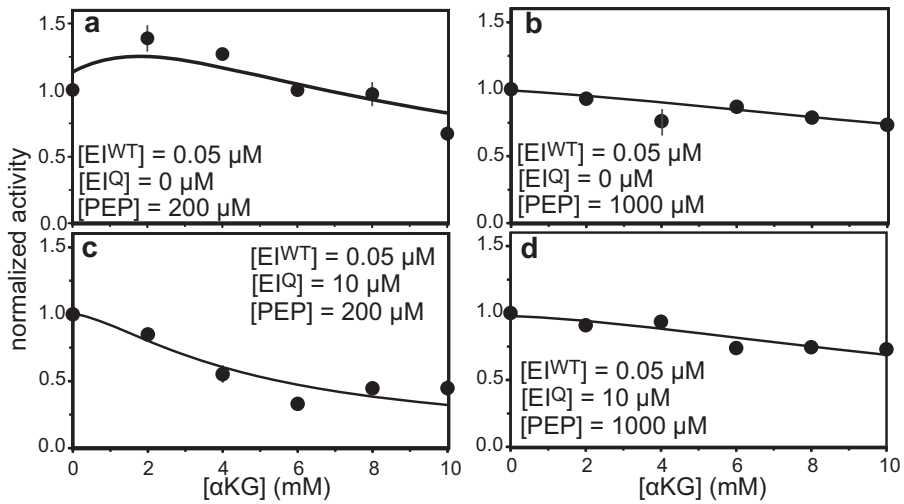

Figure 6. Dependence of the phosphoryl transfer reaction on the concentration of αKG. Enzyme kinetic data were measured at a fixed concentration of EI^{WT} (~0,05 μM). EI^{Q} and PEP concentrations were as follows: *a*, 0 μM EI^{Q} and 200 μM PEP; *b*, 0 μM EI^{Q} and 1000 μM PEP; *c*, 10 μM EI^{Q} and 200 μM PEP; *d*, 10 μM EI^{Q} and 1000 μM PEP. The data in *a*–*d* were fit using the kinetic model summarized by Equations 11–37 ("Experimental procedures"). The results of the fits are shown as *solid lines*.

fitting the dependence of the phosphoryl transfer reaction on the concentration of enzyme, the model has been simplified by setting the dissociation constant of the EI dimer occupied by a single ligand molecule to $K_{D,free}$ (see Equations 21–37 under "Experimental procedures"). Fits were performed by keeping K_m, K_I, and $K_{D,free}$ to their measured values (300, 2200, and 1 μM, respectively) (5), and optimizing values for $K_{D,bound}$ and k_{phosp}. In all cases, a $K_{D,bound}$ of $<10^{-7}$ M was obtained.

The kinetic model summarized by Equations 21–37 was used to simulate the effect of physiological fluctuations in the intracellular environment on the activity of αKG against EI (Fig. 7). In this simulation, K_m and K_I were set to the literature values for

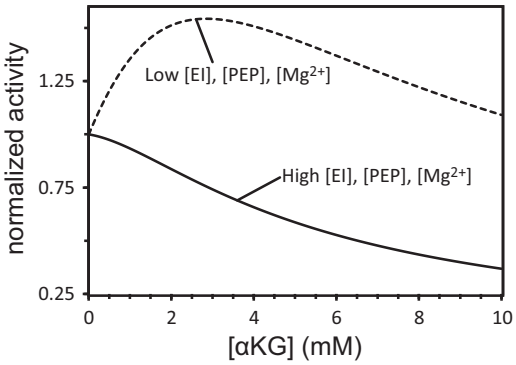

Figure 7. Effect of physiological fluctuations of the intracellular environment on the activity of αKG against EI. The rate of the phosphoryl transfer reaction is simulated in DynaFit 4.0 (23) using the kinetic model summarized by equations 18–32. K_m, K_I, and $K_{D,\text{bound}}$ were set to 300 μM (5), 2200 μM (5), and 10^{-7} M (this work), respectively. The concentration of EI was set to 0.5 μM (*dashed line*) or 10 μM (*solid line*) (16). PEP concentration was 30 μM (*dashed line*) or 300 μM (*solid line*) (14, 15). The value of $K_{D,\text{free}}$ depends on the concentration of Mg^{2+}. Here, a $K_{D,\text{free}}$ of 5 μM (*dashed line*) or 1 μM (*solid line*) was used to simulate an intracellular environment poor (~0.1 mM) or rich (~4 mM) of Mg^{2+}, respectively (8).

the EI–PEP and EI–αKG interactions (5), respectively. $K_{D,\text{bound}}$ was set to 10^{-7} M, the upper bound value obtained by fitting the enzyme kinetic data in Figs. 4 and 6 (this work). The intracellular concentrations of EI, PEP, and αKG were considered to vary in the 0.5–10 μM (16), 30–300 μM (14, 15), and 0–10 mM (4) range, respectively. $K_{D,\text{free}}$ is strongly affected by the presence of divalent cations in the buffer (8). Therefore, $K_{D,\text{free}}$ was set to 5 or 1 μM (8) to simulate low (0.1 mM) or high (4 mM) intracellular concentration of free Mg^{2+}, respectively. Our simulation (Fig. 7) suggests that αKG binding can provide up to 1.5 times stimulation of EI activity at physiological conditions that promote the monomeric form of the enzyme (low concentrations of EI, PEP, and Mg^{2+}) but results in strong inhibition of enzymatic activity at physiological concentrations of EI, PEP, and Mg^{2+} that stabilize the EI dimer.

Discussion

In this work, we describe a novel method based on fast NMR techniques to assay the activity of EI under a wide range of experimental conditions. Previously reported methods to assay the activity of EI required quantification by mass spectrometry of pyruvate (formed as a by-product of the phosphoryl transfer reaction) (4) or quantification of phosphohistidine containing proteins (either EI or some other PTS component) by radioactive labeling (24, 25) or by using a recently developed antibody (26). Compared with these methods, our protocol allows for observation of the phosphoryl transfer reaction in real time, therefore reducing the number of reagents and experimental steps required by the assay. On the other hand, our approach does not allow to monitor multiple reactions (*i.e.* multiple substrate concentrations) simultaneously and can only be applied if a 10% (or larger) reduction in NMR signal intensity is obtained for unphosphorylated HPr upon phosphorylation. This latter condition implies that phosphoryl transfer kinetics at concentrations of PEP lower than 100 μM cannot be characterized accurately by our approach.

Using our NMR-based assay, we show that the small molecule metabolite αKG can act either as an allosteric stimulator or as a competitive inhibitor of EI depending on the oligomeric state of the enzyme (Figs. 5 and 6). Indeed, at experimental conditions favoring the dimeric form of EI, αKG inhibits the phosphoryl transfer activity of the enzyme (Fig. 6, *b–d*). In contrast, at experimental conditions favoring monomeric EI, addition of αKG results in a shift of the monomer–dimer equilibrium toward the enzymatically active dimeric form and a consequential stimulation of enzymatic activity (Fig. 6*a*). Interestingly, the intracellular concentration of EI was measured to be close to the equilibrium dissociation constant for protein dimerization (16), and the dimer K_D of the free enzyme was shown to be affected substantially by varying the concentration of Mg^{2+} in the experimental buffer (from 5 to 1 μM moving from 0 to 4 mM Mg^{2+}) (8). In addition, the intracellular amount of PEP and αKG are close to the dissociation constants for PEP and αKG binding to the enzyme, respectively (4, 14, 15). In this scenario, small fluctuations in the intracellular concentrations of EI, Mg^{2+}, PEP, and αKG induced by a change in the extracellular environment would drastically affect the activity of αKG on the PTS (Fig. 7). The PTS plays multiple regulatory functions in bacterial metabolism (including sugar uptake, virulence, biofilm formation, and chemotaxis) (1–3). These PTS-mediated regulatory mechanisms are based either on direct phosphorylation of the target protein by one of the PTS components or on phosphorylation-dependent interactions (2). Therefore, the interplay between allosteric stimulation and competitive inhibition of EI by αKG revealed here may be required to tune the phosphorylation state of PTS in response to a change in the extracellular environment. Although the inhibitory activity of αKG on EI has been already proven to regulate the uptake of PTS sugars by bacterial cells in response to the availability of nitrogen source (4), understanding the effect of the weak stimulatory activity of αKG at low concentration of PEP on the biology of bacterial cells will require further investigations. Finally, this work shows how the activity of small molecule metabolites against their biological targets can change significantly in response to small changes in experimental conditions and illustrates that the dependence of the oligomeric state of the enzyme on the experimental conditions must be considered with great care when interpreting enzyme kinetic data.

Experimental procedures

Protein expression and purification

Uniformly ^{15}N-labeled *E. coli* HPr was expressed and purified as previously described (27). The H189Q (EI^Q) mutant of *E. coli* EI was created using the QuikChange site-directed mutagenesis kit (Stratagene). Genes for EI and EI^Q were cloned into a pET-15b vector (Novagen) incorporating a N-terminal His tag. The plasmid was introduced into *E. coli* strain BL21star(DE3) (Invitrogen), and the transformed bacteria were plated onto an LB-agar plate containing ampicillin (100 μg/ml) for selection. Cells were grown at 37 °C in LB medium. At A_{600} of ~0.4, the temperature was reduced to 20 °C, and expression was induced with 1 mM isopropyl-D-thiogalactopyranoside. The cells were harvested by centrifugation (4,000 × *g* for 30 min) after 16 h of induction, and the pellet was resuspended in 20 ml of 20 mM Tris, pH 8.0 (buffer A). The suspension was

lysed using a microfluidizer and centrifuged at 40,000 × *g* for 40 min. The supernatant was filtrated through a 0.45-μm filter membrane to remove cell debris and applied to a His affinity column (GE Healthcare). After the sample was loaded, the column was washed with buffer B (buffer A containing 20 mM imidazole), and the target protein was eluted with buffer C (buffer A containing 300 mM imidazole). The fractions containing the protein were confirmed by SDS-polyacrylamide gel electrophoresis and farther purified by gel filtration on a Superdex 200 column (GE Healthcare) equilibrated with 20 mM Tris, pH 7.4, 200 mM NaCl, 2 mM DTT, and 1 mM EDTA. Relevant fractions were loaded on an EnrichQ anion exchange column (Bio-Rad), and the protein was eluted with a 400-ml gradient from 150 mM to 400 mM NaCl.

Analytical ultracentrifugation

Sedimentation velocity experiments were carried out on a Beckman Coulter ProteomeLab XL-I analytical ultracentrifuge at 50 kilo-revolutions per minute and 20 °C following standard protocols (28). A 2.0 mM stock solution of EI was diluted 50-fold in 100 mM NaCl, 20 mM Tris buffer, pH 7.4, 2 mM DTT, and 1 mM EDTA (buffer A) and used to prepare a series of solutions ranging from ~1 to 40 μM by serial dilution. Samples were loaded into two-channel epon centerpiece cells (12- or 3-mm path length depending on the concentration). Absorbance (280 nm) and Rayleigh interference (655 nm) scans were collected, time-corrected (29), and analyzed in SEDFIT 15.01c (30) in terms a continuous *c*(*s*) distribution covering an *s* range of 0.0–10.0 S with a resolution of 200 and a maximum entropy regularization confidence level of 0.68. Good fits were obtained with root mean square deviation values corresponding to typical instrumental noise values. Identical experiments were carried out in buffer A containing 20 mM PEP (buffer B) or 20 mM αKG (buffer C). Weighted-average sedimentation coefficients obtained by integration of the c(*s*) distributions for EI in buffer A were used to create an isotherm that was analyzed in SEPDPHAT 13.0a in terms of a reversible monomer–dimer equilibrium to obtain a K_d of 1 μM, which is consistent with previous investigations of the EI monomer–dimer equilibrium (5, 8). The solution density (ρ) and viscosity (η) for buffer A were calculated based on the solvent composition using SEDNTERP (31). Solution densities for buffers B and C were measured at 20 °C on an Anton–Paar DMA 5000 density meter; solution viscosities were measured at 20 °C using an Anton–Paar AMVn rolling ball viscometer. The partial specific volume (*v*) and absorption extinction coefficient for EI were calculated in SEDNTERP (31) based on the amino acid composition. The corresponding interference signal increment (32) was calculated in SEDFIT15.01c (30).

Enzyme kinetic assay

The ability of EI to transfer the phosphoryl group from PEP to HPr was assayed at 37 °C using fast NMR methods (21) as described under "Results." NMR spectra were recorded on a Bruker 700 MHz spectrometer equipped with a z-shielded gradient triple resonance cryoprobe. The spectra were processed using NMRPipe (33) and analyzed using the program SPARKY (http://www.cgl.ucsf.edu/home/sparky).[3] The ^{1}H-^{15}N correlation spectrum of unphosphorylated HPr was assigned according to previously reported chemical shift tables (34). Composition of the reaction buffer was as follow: 20 mM Tris, pH 7.4, 100 mM NaCl, 4 mM $MgCl_2$, 2 mM DTT, 1 mM EDTA, and 95% H_2O/5% D_2O (v/v). Unless stated otherwise, all enzymatic assays were run in a reaction volume of 500 μl and at fixed concentrations of wildtype EI (~0.05 μM) and HPr (1 mM). The assays were run in triplicate. The initial velocities for the phosphoryl transfer reaction in the presence of different amount of EI^{Q} (see "Results" and "Discussion") were fit in DynaFit 4.0 (23) using the following kinetic model,

$$E + S \Leftrightarrow ES \quad K_M \qquad \text{(Eq. 1)}$$

$$Q + S \Leftrightarrow QS \quad K_M \qquad \text{(Eq. 2)}$$

$$E + Q \Leftrightarrow EQ \quad K_{D,\text{free}} \qquad \text{(Eq. 3)}$$

$$EQ + S \Leftrightarrow EQS \quad K_M \qquad \text{(Eq. 4)}$$

$$EQ + S \Leftrightarrow ESQ \quad K_M \qquad \text{(Eq. 5)}$$

$$EQS + S \Leftrightarrow ESQS \quad K_M \qquad \text{(Eq. 6)}$$

$$ESQ + S \Leftrightarrow ESQS \quad K_M \qquad \text{(Eq. 7)}$$

$$E + QS \Leftrightarrow EQS \quad K_{D,\text{free}} \qquad \text{(Eq. 8)}$$

$$ES + Q \Leftrightarrow ESQ \quad K_{D,\text{free}} \qquad \text{(Eq. 9)}$$

$$ES + QS \Leftrightarrow ESQS \quad K_{D,\text{bound}} \qquad \text{(Eq. 10)}$$

$$ESQS \Rightarrow EQS + P \quad k_{\text{phosp}} \qquad \text{(Eq. 11)}$$

$$ESQ \Rightarrow EQ + P \quad k_{\text{phosp}} \qquad \text{(Eq. 12)}$$

where *E* is the wildtype enzyme (EI^{WT}), *Q* is the concentration of EI^{Q}, *S* is the substrate (PEP), *ES* is the EI^{WT}-PEP complex, *QS* is the EI^{Q}-PEP complex, *EQ* is the mixed $EI^{WT}E^{Q}$ dimer, *EQS* is the mixed dimer with PEP bound to the EI^{Q} subunit, *ESQ* is the mixed dimer with PEP bound to the EI^{WT} subunit, *ESQS* is the mixed dimer with two PEP molecules, *P* is the product, $K_{D,\text{free}}$ (1 μM) is the dimer dissociation constant for free EI, $K_{D,\text{bound}}$ (fitted) is the dimer dissociation constant for EI when saturated with ligands, K_m (300 μM) is the Michaelis constant for the EI–PEP interaction, k_{phosp} (fitted) is the rate constant for the phosphoryl transfer interaction, [dharrow] indicates a thermodynamic equilibrium, and → indicates the unidirectional chemical step. Note that given the small amount of EI^{WT} compared with EI^{Q}, the amount of $EI^{WT}EI^{WT}$ dimer is considered to be negligible in this model.

The initial velocities for the phosphoryl transfer reaction in the presence of different amount of PEP (see "Results" and "Discussion") were fit in DynaFit 4.0 (23) using the following kinetic model,

$$E + S \Leftrightarrow ES \quad K_M \qquad \text{(Eq. 13)}$$

$$E + E \Leftrightarrow E_2 \quad K_{D,\text{free}} \qquad \text{(Eq. 14)}$$

[3] Please note that the JBC is not responsible for the long-term archiving and maintenance of this site or any other third party hosted site.

$$E_2 + S \Leftrightarrow E_2S \quad K_M \qquad \text{(Eq. 15)}$$

$$E_2S + S \Leftrightarrow E_2S_2 \quad K_M \qquad \text{(Eq. 16)}$$

$$E + ES \Leftrightarrow E_2S \quad K_{D,\text{free}} \qquad \text{(Eq. 17)}$$

$$ES + ES \Leftrightarrow E_2S_2 \quad K_{D,\text{bound}} \qquad \text{(Eq. 18)}$$

$$E_2S_2 \Rightarrow E_2S + P \quad k_{\text{phosp}} \qquad \text{(Eq. 19)}$$

$$E_2S \Rightarrow E_2 + P \quad k_{\text{phosp}} \qquad \text{(Eq. 20)}$$

where E_2 is the $EI^{WT}EI^{WT}$ dimer, E_2S is the EI dimer complexed to one molecule of PEP, and E_2S_2 is the dimer complexed with two molecules of PEP.

Enzyme kinetic data measured at different concentration of αKG were fit in DynaFit 4.0 (23) using the following kinetic model,

$$E + S \Leftrightarrow ES \quad K_M \qquad \text{(Eq. 21)}$$

$$E + I \Leftrightarrow EI \quad K_I \qquad \text{(Eq. 22)}$$

$$E + E \Leftrightarrow E_2 \quad K_{D,\text{free}} \qquad \text{(Eq. 23)}$$

$$E_2 + S \Leftrightarrow E_2S \quad K_M \qquad \text{(Eq. 24)}$$

$$E_2S + S \Leftrightarrow E_2S_2 \quad K_M \qquad \text{(Eq. 25)}$$

$$E_2 + I \Leftrightarrow E_2I \quad K_I \qquad \text{(Eq. 26)}$$

$$E_2I + I \Leftrightarrow E_2I_2 \quad K_I \qquad \text{(Eq. 27)}$$

$$E_2I + S \Leftrightarrow E_2SI \quad K_M \qquad \text{(Eq. 28)}$$

$$E_2S + I \Leftrightarrow E_2SI \quad K_I \qquad \text{(Eq. 29)}$$

$$E + ES \Leftrightarrow E_2S \quad K_{D,\text{free}} \qquad \text{(Eq. 30)}$$

$$ES + ES \Leftrightarrow E_2S_2 \quad K_{D,\text{bound}} \qquad \text{(Eq. 31)}$$

$$E + EI \Leftrightarrow E_2I \quad K_{D,\text{free}} \qquad \text{(Eq. 32)}$$

$$EI + EI \Leftrightarrow E_2I_2 \quad K_{D,\text{bound}} \qquad \text{(Eq. 33)}$$

$$ES + EI \Leftrightarrow E_2SI \quad K_{D,\text{bound}} \qquad \text{(Eq. 34)}$$

$$E_2S_2 \Rightarrow E_2S + P \quad k_{\text{phosp}} \qquad \text{(Eq. 35)}$$

$$E_2S \Rightarrow E_2 + P \quad k_{\text{phosp}} \qquad \text{(Eq. 36)}$$

$$E_2SI \Rightarrow E_2I + P \quad k_{\text{phosp}} \qquad \text{(Eq. 37)}$$

where I is the inhibitor (αKG), EI is the EI–αKG complex, E_2I is the EI dimer complexed with one αKG molecule, E_2I_2 is the EI dimer complexed with two αKG molecules, E_2SI is the EI dimer complexed with one αKG molecule and one PEP molecule, and K_I (2.2 mM) is the dissociation constant for free EI–αKG interaction. In the fits, the concentration of EI is considered to be the sum of the active (EI^{WT}) and inactive (EI^{Q}) species.

Author contributions—T. T. N., R. G., and V. V. data curation; T. T. N., R. G., and V. V. formal analysis; T. T. N. and V. V. writing-original draft; T. T. N., R. G., and V. V. writing-review and editing; R. G. and V. V. funding acquisition; V. V. conceptualization; V. V. supervision.

Acknowledgment—We thank Dr. Scott Nelson for helpful discussions.

References

1. Clore, G. M., and Venditti, V. (2013) Structure, dynamics and biophysics of the cytoplasmic protein–protein complexes of the bacterial phosphoenolpyruvate: sugar phosphotransferase system. *Trends Biochem. Sci.* **38,** 515–530 CrossRef Medline
2. Deutscher, J., Aké, F. M., Derkaoui, M., Zébré, A. C., Cao, T. N., Bouraoui, H., Kentache, T., Mokhtari, A., Milohanic, E., and Joyet, P. (2014) The bacterial phosphoenolpyruvate:carbohydrate phosphotransferase system: regulation by protein phosphorylation and phosphorylation-dependent protein-protein interactions. *Microbiol. Mol. Biol. Rev.* **78,** 231–256 CrossRef Medline
3. Postma, P. W., Lengeler, J. W., and Jacobson, G. R. (1996) Phosphoenolpyruvate:carbohydrate phosphotransferase systems. In *Escherichia coli and Salmonella: Cellular and Molecular Biology* (Neidhardt, F. C., Lin, E. C., and Curtiss, R., eds) pp. 1149–1174, ASM Press, Washington, D. C.
4. Doucette, C. D., Schwab, D. J., Wingreen, N. S., and Rabinowitz, J. D. (2011) α-Ketoglutarate coordinates carbon and nitrogen utilization via enzyme I inhibition. *Nat. Chem. Biol.* **7,** 894–901 CrossRef Medline
5. Venditti, V., Ghirlando, R., and Clore, G. M. (2013) Structural basis for enzyme I inhibition by α-ketoglutarate. *ACS Chem. Biol.* **8,** 1232–1240 CrossRef Medline
6. Hogema, B. M., Arents, J. C., Bader, R., Eijkemans, K., Yoshida, H., Takahashi, H., Aiba, H., and Postma, P. W. (1998) Inducer exclusion in *Escherichia coli* by non-PTS substrates: the role of the PEP to pyruvate ratio in determining the phosphorylation state of enzyme IIAGlc. *Mol. Microbiol.* **30,** 487–498 CrossRef Medline
7. Chauvin, F., Brand, L., and Roseman, S. (1996) Enzyme I: the first protein and potential regulator of the bacterial phosphoenolpyruvate: glycose phosphotransferase system. *Res. Microbiol.* **147,** 471–479 CrossRef Medline
8. Patel, H. V., Vyas, K. A., Savtchenko, R., and Roseman, S. (2006) The monomer/dimer transition of enzyme I of the *Escherichia coli* phosphotransferase system. *J. Biol. Chem.* **281,** 17570–17578 CrossRef Medline
9. Venditti, V., and Clore, G. M. (2012) Conformational selection and substrate binding regulate the monomer/dimer equilibrium of the C-terminal domain of *Escherichia coli* enzyme I. *J. Biol. Chem.* **287,** 26989–26998 CrossRef Medline
10. Teplyakov, A., Lim, K., Zhu, P. P., Kapadia, G., Chen, C. C., Schwartz, J., Howard, A., Reddy, P. T., Peterkofsky, A., and Herzberg, O. (2006) Structure of phosphorylated enzyme I, the phosphoenolpyruvate:sugar phosphotransferase system sugar translocation signal protein. *Proc. Natl. Acad. Sci. U.S.A.* **103,** 16218–16223 CrossRef Medline
11. Venditti, V., Tugarinov, V., Schwieters, C. D., Grishaev, A., and Clore, G. M. (2015) Large interdomain rearrangement triggered by suppression of micro- to millisecond dynamics in bacterial enzyme I. *Nat. Commun.* **6,** 5960 CrossRef Medline
12. Venditti, V., Schwieters, C. D., Grishaev, A., and Clore, G. M. (2015) Dynamic equilibrium between closed and partially closed states of the bacterial enzyme I unveiled by solution NMR and X-ray scattering. *Proc. Natl. Acad. Sci. U.S.A.* **112,** 11565–11570 CrossRef Medline
13. Seok, Y. J., Zhu, P. P., Koo, B. M., and Peterkofsky, A. (1998) Autophosphorylation of enzyme I of the *Escherichia coli* phosphoenolpyruvate: sugar phosphotransferase system requires dimerization. *Biochem. Biophys. Res. Commun.* **250,** 381–384 CrossRef Medline
14. Albe, K. R., Butler, M. H., and Wright, B. E. (1990) Cellular concentrations of enzymes and their substrates. *J. Theor. Biol.* **143,** 163–195 CrossRef Medline
15. Lagunas, R., and Gancedo, C. (1983) Role of phosphate in the regulation of the Pasteur effect in Saccharomyces cerevisiae. *Eur. J. Biochem.* **137,** 479–483 CrossRef Medline
16. Mattoo, R. L., and Waygood, E. B. (1983) Determination of the levels of HPr and enzyme I of the phosphoenolpyruvate-sugar phosphotransferase system in *Escherichia coli* and *Salmonella typhimurium*. *Can J. Biochem. Cell Biol.* **61,** 29–37 CrossRef Medline

17. Cabrera, R., Baez, M., Pereira, H. M., Caniuguir, A., Garratt, R. C., and Babul, J. (2011) The crystal complex of phosphofructokinase-2 of *Escherichia coli* with fructose-6-phosphate: kinetic and structural analysis of the allosteric ATP inhibition. *J. Biol. Chem.* **286,** 5774–5783 CrossRef Medline
18. Pervushin, K., Riek, R., Wider, G., and Wüthrich, K. (1997) Attenuated T2 relaxation by mutual cancellation of dipole-dipole coupling and chemical shift anisotropy indicates an avenue to NMR structures of very large biological macromolecules in solution. *Proc. Natl. Acad. Sci. U.S.A.* **94,** 12366–12371 CrossRef Medline
19. Weigel, N., Powers, D. A., and Roseman, S. (1982) Sugar transport by the bacterial phosphotransferase system: primary structure and active site of a general phosphocarrier protein (HPr) from *Salmonella typhimurium*. *J. Biol. Chem.* **257,** 14499–14509 Medline
20. Klumpp, S., and Krieglstein, J. (2002) Phosphorylation and dephosphorylation of histidine residues in proteins. *Eur. J. Biochem.* **269,** 1067–1071 CrossRef Medline
21. Schanda, P., Kupce, E., and Brutscher, B. (2005) SOFAST-HMQC experiments for recording two-dimensional heteronuclear correlation spectra of proteins within a few seconds. *J. Biomol. NMR* **33,** 199–211 CrossRef Medline
22. Takayama, Y., Schwieters, C. D., Grishaev, A., Ghirlando, R., and Clore, G. M. (2011) Combined use of residual dipolar couplings and solution X-ray scattering to rapidly probe rigid-body conformational transitions in a non-phosphorylatable active-site mutant of the 128 kDa enzyme I dimer. *J. Am. Chem. Soc.* **133,** 424–427 CrossRef Medline
23. Kuzmic, P. (2009) DynaFit: a software package for enzymology. *Methods Enzymol.* **467,** 247–280 CrossRef Medline
24. Meadow, N. D., Mattoo, R. L., Savtchenko, R. S., and Roseman, S. (2005) Transient state kinetics of enzyme I of the phosphoenolpyruvate:glycose phosphotransferase system of *Escherichia coli*: equilibrium and second-order rate constants for the phosphotransfer reactions with phosphoenolpyruvate and HPr. *Biochemistry* **44,** 12790–12796 CrossRef Medline
25. Lee, C. R., Park, Y. H., Kim, M., Kim, Y. R., Park, S., Peterkofsky, A., and Seok, Y. J. (2013) Reciprocal regulation of the autophosphorylation of enzyme INtr by glutamine and α-ketoglutarate in *Escherichia coli*. *Mol. Microbiol.* **88,** 473–485 CrossRef Medline
26. Kee, J. M., Oslund, R. C., Perlman, D. H., and Muir, T. W. (2013) A pan-specific antibody for direct detection of protein histidine phosphorylation. *Nat. Chem. Biol.* **9,** 416–421 CrossRef Medline
27. Suh, J. Y., Cai, M., and Clore, G. M. (2008) Impact of phosphorylation on structure and thermodynamics of the interaction between the N-terminal domain of enzyme I and the histidine phosphocarrier protein of the bacterial phosphotransferase system. *J. Biol. Chem.* **283,** 18980–18989 CrossRef Medline
28. Zhao, H., Brautigam, C. A., Ghirlando, R., and Schuck, P. (2013) Overview of current methods in sedimentation velocity and sedimentation equilibrium analytical ultracentrifugation. *Curr. Protoc. Protein Sci.* Chapter 20, Unit 20.12
29. Ghirlando, R., Balbo, A., Piszczek, G., Brown, P. H., Lewis, M. S., Brautigam, C. A., Schuck, P., and Zhao, H. (2013) Improving the thermal, radial, and temporal accuracy of the analytical ultracentrifuge through external references. *Anal. Biochem.* **440,** 81–95 CrossRef Medline
30. Schuck, P. (2000) Size-distribution analysis of macromolecules by sedimentation velocity ultracentrifugation and lamm equation modeling. *Biophys. J.* **78,** 1606–1619 CrossRef Medline
31. Cole, J. L., Lary, J. W., Moody, T., Laue, T. M. (2008) Analytical ultracentrifugation: sedimentation velocity and sedimentation equilibrium. *Methods Cell Biol.* **84,** 143–179 CrossRef Medline
32. Zhao, H., Brown, P. H., and Schuck, P. (2011) On the distribution of protein refractive index increments. *Biophys. J.* **100,** 2309–2317 CrossRef Medline
33. Delaglio, F., Grzesiek, S., Vuister, G. W., Zhu, G., Pfeifer, J., and Bax, A. (1995) NMRPipe: a multidimensional spectral processing system based on UNIX pipes. *J. Biomol. NMR* **6,** 277–293 Medline
34. Garrett, D. S., Seok, Y. J., Peterkofsky, A., Gronenborn, A. M., and Clore, G. M. (1999) Solution structure of the 40,000 Mr phosphoryl transfer complex between the N-terminal domain of enzyme I and HPr. *Nat. Struct. Biol.* **6,** 166–173 CrossRef Medline

The oligomerization state of bacterial enzyme I (EI) determines EI's allosteric stimulation or competitive inhibition by α-ketoglutarate

Trang T. Nguyen, Rodolfo Ghirlando and Vincenzo Venditti

J. Biol. Chem. 2018, 293:2631-2639.
doi: 10.1074/jbc.RA117.001466 originally published online January 9, 2018